Extensions of the tetrahedron method for evaluating spectral properties of solids

1979 J. Phys. C: Solid State Phys. 12 2991

(http://iopscience.iop.org/0022-3719/12/15/008)

J. Phys. C: Solid State Phys., Vol. 12, 1979. Printed in Great Britain. © 1979

Extensions of the tetrahedron method for evaluating spectral properties of solids

A H MacDonald†‡, S H Vosko† and P T Coleridge§

† Department of Physics, University of Toronto, Toronto, Canada M5S 1A7

§ Division of Physics, National Research Council of Canada, Ottawa, Canada K1K 3Y3

Received 6 November 1978, in final form 25 January 1979

Abstract. Two extensions of the widely used tetrahedron method for the evaluation of spectral properties of solids are presented. The first provides explicit formulae for including matrix element variation inside tetrahedral microzones in the same spirit in which the energy variation is included in the original method. The second is a scheme for using local quadratic interpolation inside some tetrahedra to provide the matrix element and energy values required to apply the tetrahedron method to a large number of tetrahedra into which the original tetrahedra have been divided. This scheme is similar to the hybrid method extension of the Gilat–Raubenheimer method. Application to the calculation of the density of states of a single tight-binding band in a FCC crystal shows that its efficiency is comparable with that of the method recently proposed by Chen.

1. Introduction

The importance of efficient techniques for Brillouin zone (BZ) integrations in solid-state physics has been widely appreciated in recent years. (For a review of the topic see Gilat 1972, 1976.) Such techniques are of great importance in self-consistent band calculations (e.g. see Wang and Callaway 1977) as well as in the calculation of such crystal properties as optical spectra and susceptibility functions. Most Brillouin zone integrals of interest are simply related to that for a general spectral function which is of the form

$$G(\omega) = \int_{\mathrm{BZ}} \frac{\mathrm{d}\boldsymbol{k}\, F(\boldsymbol{k})}{(\omega - \omega(\boldsymbol{k}) - \mathrm{i}\epsilon)} \tag{1.1}$$

where ϵ is a positive infinitesimal, the $\omega(\boldsymbol{k})$ are eigenvalues for some elementary excitation and $F(\boldsymbol{k})$ is some matrix element. Usually the BZ integrals can be restricted by symmetry to an irreducible region of the BZ. The real and imaginary parts of $G(\omega)$ are

$$R(\omega) = \int \frac{\mathrm{d}\boldsymbol{k}\, F(\boldsymbol{k})}{(\omega - \omega(\boldsymbol{k}))} \tag{1.2}$$

and

$$\pi I(\omega) = \pi \int \mathrm{d}\boldsymbol{k}\, F(\boldsymbol{k}) \delta(\omega - \omega(\boldsymbol{k})) \tag{1.3}$$

respectively. Since $R(\omega)$ and $I(\omega)$ are related by Kramers–Krönig relations it is sufficient to restrict our attention to $I(\omega)$. The techniques discussed below can, however, be

‡ Present address: Division of Physics, NRC of Canada, Ottawa, Canada K1A OR6

modified to evaluate $R(\omega)$ directly. (Compare §§ 2 and 3 with Rath and Freeman (1975).) Also of great interest is the integrated function

$$J(\omega) = \int_{-\infty}^{\omega} \mathrm{d}\omega' I(\omega') = \int_{\mathrm{BZ}} \mathrm{d}\boldsymbol{k}\, F(\boldsymbol{k})\theta(\omega - \omega(\boldsymbol{k})). \tag{1.4}$$

The charge density of a solid is an example of a quantity expressed by a BZ integral of the form of equation (1.4).

When $F(\boldsymbol{k}) = 1$ in equation (1.3), $I(\omega)$ reduces to the familiar density-of-states function $g(\omega)$. Gilat (1972) has examined in detail the evaluation of $g(\omega)$ and has distinguished five separate methods: (i) the root-sampling method (Blackman 1937, Brust 1968); (ii) the linear discrete method (Gilat and Dolling 1964); (iii) the quadratic discrete method (Mueller *et al* 1971); (iv) the Gilat–Raubenheimer (1966) method and (v) the hybrid method (Janak *et al* 1970, Cooke and Wood 1972). Gilat's analysis shows that the last two of these methods are clearly superior. Subsequently the tetrahedron method (Jepsen and Andersen 1971, Lehmann and Taut 1972) and the ray method (Chen 1977) have been proposed. The choice between these last four methods in practice depends on a variety of considerations including the desired accuracy, the ease of application, the importance of an accurate treatment of Van Hove singularities and the complexity of the evaluation of $\omega(\boldsymbol{k})$ and $F(\boldsymbol{k})$. Detailed comparisons are contained in several of the papers quoted above and will not be repeated here. The tetrahedron method is frequently a good choice and is one of the most extensively used. In this paper we present equations which represent a generalisation of the original tetrahedron method and suggest a hybrid tetrahedron method which is analogous to the hybrid Gilat–Raubenheimer methods. The relation of this hybrid method to the other methods mentioned above is discussed in the next paragraph. Section 2 reviews the original tetrahedron method and describes its generalisation to the $F(\boldsymbol{k})$ not constant case. In § 3 the hybrid tetrahedron method is described and the results of its application to the calculation of $g(\omega)$ for a single tight-binding band of an FCC crystal are shown as a demonstration of its usefulness. Section 4 contains concluding remarks.

The Gilat–Raubenheimer method (1966) is based on the division of the BZ (or the irreducible region) into a large number of cubic microzones, usually of equal volume, inside which $\omega(\boldsymbol{k})$ is approximated by a linear form. The contribution to $g(\omega)$ and $n(\omega) \equiv \int_{-\infty}^{\omega} \mathrm{d}\omega' g(\omega')$ from each microzone can then be evaluated analytically. The tetrahedron method is similar but the microzones are general tetrahedra rather than cubes. A problem with both these methods is that the convergence with the number of microzones, N, is not rapid. (In fact the error is roughly proportional to $N^{-2/3}$.) More rapid convergence with increasing numbers of microzones was obtained in the approach of Mueller *et al* (1971) which is based on a quadratic form approximation for $\omega(\boldsymbol{k})$ inside each cubic microzone and the root-sampling method. For this reason Cooke *et al* (1972) and Janak *et al* (1970) suggested the hybrid method in which the quadratic form for $\omega(\boldsymbol{k})$ is used to define a linear form for $\omega(\boldsymbol{k})$ inside still smaller cubic microzones. Then the Gilat–Raubenheimer method can be used to calculate $g(\omega)$. The hybrid tetrahedron method described in this paper, is analogous to these hybrid methods but is in the context of the tetrahedron method rather than the Gilat–Raubenhemier method.

2. The inclusion of matrix element variation in the tetrahedron method

In the original tetrahedron method (Jepsen *et al* 1971, Lehmann *et al* 1972) the linear form used for $\omega(\boldsymbol{k})$ is the unique result of linear interpolation which matches the exact

values at the four tetrahedron vertices. If the $\boldsymbol{k}$-dependence of $F(\boldsymbol{k})$ is to be included in the scheme, the consistent approximation is to replace $F(\boldsymbol{k})$ as well by the result of linear interpolation which matches at the tetrahedron vertices. We label the energies at the vertices of the ith tetrahedron ω_1^i, ω_2^i, ω_3^i, and ω_4^i ($\omega_k^i \leqslant \omega_{k+1}^i$) and the matrix element values F_1^i, F_2^i, F_3^i and F_4^i. It is an important simplification of the tetrahedron method that the expressions we will derive for $g(\omega)$, $n(\omega)$, $I(\omega)$ and $J(\omega)$ are dependent only on ω and the above eight quantities; they are entirely independent of the shapes of the tetrahedral microzones. Expressions for the inclusion of matrix element variations in the calculation by $I(\omega)$ by the tetrahedron method have been given previously by Gilat and Bharatiya (1975). The corresponding expressions required for the evaluation of $J(\omega)$ are given here for the first time.

To define notation we write

$$g(\omega) = V_{\mathrm{MZ}} \sum_{i=1}^{N} g(\omega, \omega_1^i, \omega_2^i, \omega_3^i, \omega_4^i) \equiv V_{\mathrm{MZ}} \sum_{i=1}^{N} g^i \tag{2.1a}$$

$$n(\omega) = V_{\mathrm{MZ}} \sum_{i=1}^{N} n(\omega, \omega_1^i, \omega_2^i, \omega_3^i, \omega_4^i) \equiv V_{\mathrm{MZ}} \sum_{i=1}^{N} n^i \tag{2.1b}$$

$$I(\omega) = V_{\mathrm{MZ}} \sum_{i=1}^{N} g^i \sum_{k=1}^{4} I_k(\omega, \omega_1^i, \omega_2^i, \omega_3^i, \omega_4^i) F_k^i \equiv V_{\mathrm{MZ}} \sum_{i=1}^{N} g^i \sum_{k=1}^{4} I_k^i F_k^i \tag{2.1c}$$

$$J(\omega) = V_{\mathrm{MZ}} \sum_{i=1}^{N} n^i \sum_{k=1}^{4} J_k(\omega, \omega_1^i, \omega_2^i, \omega_3^i, \omega_4^i) F_k^i \equiv V_{\mathrm{MZ}} \sum_{i=1}^{N} n^i \sum_{k=1}^{4} J_k^i F_k^i \tag{2.1d}$$

where N is the number of tetrahedral microzones and V_{MZ} is the microzone volume. The required expressions are most easily derived by considering $J(\omega)$ first and then differentiating with respect to ω to obtain $I(\omega)$. The expressions for $g(\omega)$ and $n(\omega)$ then follow as a special case by setting $F_k^i = 1$. Note that $\sum_{k=1}^{4} I_k^i = \sum_{k=1}^{4} J_k^i = 1$ in equations (2.1*c*) and (2.1*d*). These coefficients thus describe how the values of $F(\boldsymbol{k})$ at the tetrahedron vertices are to be averaged to obtain the appropriate contributions to $I(\omega)$ and $J(\omega)$. We must consider five separate cases:

(i) For $\omega < \omega_1^i$ the tetrahedral microzone is entirely unoccupied and there is no contribution to $g(\omega)$, $n(\omega)$, $I(\omega)$ or $J(\omega)$. (We will refer to the portion of the tetrahedron for which the linear interpolation of $\omega(\boldsymbol{k})$, $\tilde{\omega}(\boldsymbol{k})$, is less than ω as the occupied part. The tetrahedron index will be dropped wherever no confusion is likely.)

(ii) For $\omega_1^i < \omega < \omega_2^i$ the occupied portion of the tetrahedron is a tetrahedron with vertices at $\boldsymbol{k}_1$, $\boldsymbol{k}_\alpha = f_{2,1}\boldsymbol{k}_2 + f_{1,2}\boldsymbol{k}_1$, $\boldsymbol{k}_\beta = f_{3,1}\boldsymbol{k}_3 + f_{1,3}\boldsymbol{k}_1$ and $\boldsymbol{k}_\gamma = f_{4,1}\boldsymbol{k}_4 + f_{1,4}\boldsymbol{k}_1$ as shown in figure 1. We have defined

$$f_{n,m} \equiv (\omega - \omega_m)/(\omega_n - \omega_m), \tag{2.2}$$

noting that $f_{n,m} + f_{m,n} = 1$. $f_{n,m}$ is the fraction of the distance from $\boldsymbol{k}_m$ to $\boldsymbol{k}_n$ at which $\tilde{\omega}(\boldsymbol{k})$ equals ω. To evaluate the contribution to $J(\omega)$ we replace $F(\boldsymbol{k})$ by its linear interpolation $\tilde{F}(\boldsymbol{k})$. Note that $\tilde{F}(\sum_i \alpha_i \boldsymbol{k}_i) = \sum_i \alpha_i \tilde{F}(\boldsymbol{k}_i)$ and that the centroid of an arbitrary tetrahedron is located at the arithmetic mean of its four vertices, independent of the shape of the tetrahedron. Then recalling that the volume of an arbitrary tetrahedron with vertices at $\boldsymbol{x}_1$, $\boldsymbol{x}_2$, $\boldsymbol{x}_3$ and $\boldsymbol{x}_4$ is given by $(\boldsymbol{x}_2 - \boldsymbol{x}_1).((\boldsymbol{x}_3 - \boldsymbol{x}_1) \times (\boldsymbol{x}_4 - \boldsymbol{x}_1))/6$ it follows that

$$\int_{\mathrm{MZ}} \tilde{F}(\boldsymbol{k}) \theta(\omega - \tilde{\omega}(\boldsymbol{k})) = V_{\mathrm{MZ}} n^i \tilde{F}((\boldsymbol{k}_1 + \boldsymbol{k}_\alpha + \boldsymbol{k}_\beta + \boldsymbol{k}_\gamma)/4) = V_{\mathrm{MZ}} n^i \sum_{k=1}^{4} J_k^i F_k^i \tag{2.3}$$

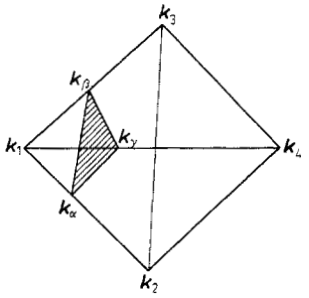

Figure 1. Intersection of a tetrahedral microzone with the planar $\tilde{\omega}(\boldsymbol{k}) = \omega$ surface for $\omega_1 < \omega < \omega_2$.

where

$$n^i = f_{2,1} f_{3,1} f_{4,1} \tag{2.4a}$$

$$J_1^i = (1 + f_{1,2} + f_{1,3} + f_{1,4})/4 \tag{2.4b}$$

and

$$J_k^i = f_{k,1}/4 \qquad k = 2, 3, 4. \tag{2.4c}$$

By differentiating equation (2.3) with respect to ω we obtain

$$g^i = 3n^i/(\omega - \omega_1) \tag{2.5a}$$

$$I_1^i = \tfrac{1}{3}(f_{1,2} + f_{1,3} + f_{1,4}) \tag{2.5b}$$

$$I_k^i = \tfrac{1}{3} f_{k,1} \qquad k = 2, 3, 4. \tag{2.5c}$$

(iii) For $\omega_2^i < \omega < \omega_3^i$ the occupied part of the tetrahedron may be considered at the sum of three tetrahedra as shown in figure 2. One tetrahedron has vertices at $\boldsymbol{k}_1, \boldsymbol{k}_2, \boldsymbol{k}_\alpha = f_{4,2}\boldsymbol{k}_4 + f_{2,4}\boldsymbol{k}_2$ and $\boldsymbol{k}_\beta = f_{3,2}\boldsymbol{k}_3 + f_{2,3}\boldsymbol{k}_2$ and volume $V_{12\alpha\beta} = V_{\mathrm{MZ}} f_{4,2} f_{3,2}$, the second has vertices at $\boldsymbol{k}_1$, $\boldsymbol{k}_\alpha$, $\boldsymbol{k}_\beta$ and $\boldsymbol{k}_\delta = f_{4,1}\boldsymbol{k}_4 + f_{1,4}\boldsymbol{k}_1$ and volume $V_{1\alpha\beta\delta} = V_{\mathrm{MZ}} f_{4,1} f_{2,4} f_{3,2}$ while the third has vertices at $\boldsymbol{k}_1$, $\boldsymbol{k}_\beta$, $\boldsymbol{k}_\delta$ and $\boldsymbol{k}_\gamma = f_{3,1}\boldsymbol{k}_3 + f_{1,3}\boldsymbol{k}_1$ and volume $V_{1\beta\delta\gamma} = f_{4,1} f_{3,1} f_{2,3}$. Expressions for J_k^i, n^i, I_k^i and g^i can be obtained exactly as in the previous

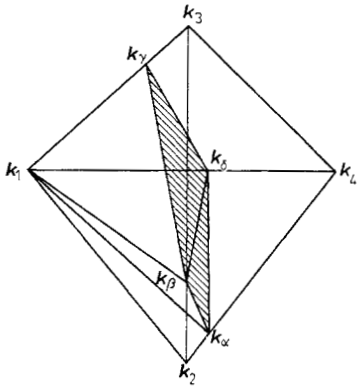

Figure 2. Intersection of a tetrahedral microzone with the planar $\tilde{\omega}(\boldsymbol{k}) = \omega$ surface for $\omega_2 < \omega < \omega_3$. The occupied portion of the tetrahedron can be divided into three non-overlapping tetrahedra with vertices at $\boldsymbol{k}_1$, $\boldsymbol{k}_2$, $\boldsymbol{k}_\alpha$ and $\boldsymbol{k}_\beta$, $\boldsymbol{k}_1$, $\boldsymbol{k}_\alpha$, $\boldsymbol{k}_\beta$ and $\boldsymbol{k}_\delta$ and $\boldsymbol{k}_1$, $\boldsymbol{k}_\beta$, $\boldsymbol{k}_\delta$ and $\boldsymbol{k}_\gamma$ respectively.

case after noting that the centroid of the occupied portion is the average of the centroids of three constituent tetrahedra weighted by their volumes. The results are rather cumbersome but may be expressed in the following form which is convenient for automatic computation.

$$n^i = f_{4,2}f_{3,2} + f_{4,1}f_{2,4}f_{3,2} + f_{4,1}f_{3,1}f_{2,3} = (V_{12\alpha\beta} + V_{1\alpha\beta\delta} + V_{1\beta\delta\gamma})/V_{MZ} \tag{2.6a}$$

$$J_1^i = (V_{12\alpha\beta} + V_{1\alpha\beta\delta}(1 + f_{1,4}) + V_{1\beta\delta\gamma}(1 + f_{1,4} + f_{1,3}))/4n^iV_{MZ} \tag{2.6b}$$

$$J_2^i = (V_{12\alpha\beta}(1 + f_{2,4} + f_{2,3}) + V_{1\alpha\beta\delta}(f_{2,4} + f_{2,3}) + V_{1\beta\delta\gamma}f_{2,3})/4n^iV_{MZ} \tag{2.6c}$$

$$J_3^i = (V_{12\alpha\beta}f_{3,2} + V_{1\alpha\beta\delta}f_{3,2} + V_{1\beta\delta\gamma}(f_{3,2} + f_{3,1}))/4n^iV_{MZ} \tag{2.6d}$$

$$J_4^i = (V_{12\alpha\beta}f_{4,2} + V_{1\alpha\beta\delta}(f_{4,2} + f_{4,1}) + V_{1\beta\delta\gamma}f_{4,1})/4n^iV_{MZ} \tag{2.6e}$$

$$g^i = 3\Delta_{4,1}^{-1}(f_{2,3}f_{3,1} + f_{3,2}f_{2,4}) \tag{2.6f}$$

$$I_1^i = f_{1,4}/3 + f_{1,3}f_{3,1}f_{2,3}/g^i\Delta_{4,1} \tag{2.6g}$$

$$I_2^i = f_{2,3}/3 + f_{2,4}^2f_{3,2}/g^i\Delta_{4,1} \tag{2.6h}$$

$$I_3^i = f_{3,2}/3 + f_{3,1}^2f_{2,3}/g^i\Delta_{4,1} \tag{2.6i}$$

$$I_4^i = f_{4,1}/3 + f_{4,2}f_{2,4}f_{3,2}/g^i\Delta_{4,1} \tag{2.6j}$$

where $\Delta_{n,m} \equiv \omega_n - \omega_m$.

(iv) For $\omega_3^i < \omega < \omega_4^i$ the occupied portion is most conveniently considered as the full tetrahedron less the tetrahedron with vertices at $\boldsymbol{k}_4$, $\boldsymbol{k}_\beta = f_{4,2}\boldsymbol{k}_4 + f_{2,4}\boldsymbol{k}_2$, $\boldsymbol{k}_\delta = f_{4,1}\boldsymbol{k}_4 + f_{1,4}\boldsymbol{k}_1$ and $\boldsymbol{k}_\gamma = f_{4,3}\boldsymbol{k}_4 + f_{3,4}\boldsymbol{k}_3$ and volume $V_{4\beta\delta\gamma} = V_{MZ}f_{1,4}f_{2,4}f_{3,4}$ (see figure 3). This leads to the expressions

$$n^i = (1 - f_{1,4}f_{2,4}f_{3,4}) \tag{2.7a}$$

$$J_1^i = (1 - f_{1,4}^2f_{2,4}f_{3,4})/4n^i \tag{2.7b}$$

$$J_2^i = (1 - f_{1,4}f_{2,4}^2f_{3,4})/4n^i \tag{2.7c}$$

$$J_3^i = (1 + f_{1,4}f_{2,4}f_{3,4}^2)/4n^i \tag{2.7d}$$

$$J_4^i = [1 - f_{1,4}f_{2,4}f_{3,4}(1 + f_{4,1} + f_{4,2} + f_{4,3})]/4n^i \tag{2.7e}$$

$$g^i = 3(1 - n^i)/(\omega_4 - \omega) \tag{2.7f}$$

$$I_n^i = f_{k,4}/3 \qquad k = 1, 2, 3 \tag{2.7g}$$

$$I_4^i = (f_{4,1} + f_{4,2} + f_{4,3})/3 \tag{2.7h}$$

(v) Finally we have the case of a full tetrahedron $\omega_4^i < \omega$. For this case there is no contribution to either $g(\omega)$ or $I(\omega)$ but

$$n^i = 1 \tag{2.8a}$$

and

$$J_k^i = \tfrac{1}{4}, \qquad k = 1, 2, 3, 4. \tag{2.8b}$$

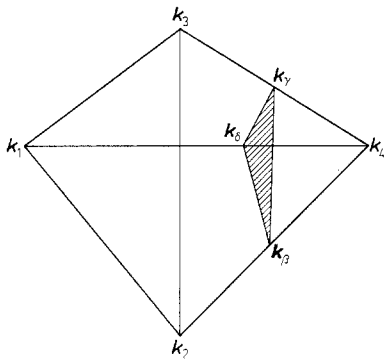

Figure 3. Intersection of the tetrahedral microzone with the planar $\tilde{\omega}(\boldsymbol{k}) = \omega$ surface for $\omega_3 < \omega < \omega_4$.

The fact that the g^i, and n^i, and particularly the I_n^i and J_k^i depend only on ω and ω_k^i is of great use in simplifying the application of this method. As ω approaches ω_1 from above, J_1 and I_1 approach one while J_2, J_3, J_4, I_2, I_3 and I_4 approach zero. This corresponds to the fact that the centroid of the occupied region of the nearly empty tetrahedron is near $\boldsymbol{k}_1$. As ω increases towards ω_4, the tetrahedron gradually fills up and all the J_k approach $\frac{1}{4}$, corresponding to the completely filled case. In this limit I_1, I_2 and I_3 approach zero while I_4 approaches one since the I coefficients average $\tilde{F}(\boldsymbol{k})$ over the $\tilde{\omega}(\boldsymbol{k}) = \omega$ plane. The way in which these coefficients vary as a tetrahedral microzone is filled is illustrated for the case $\omega_1 = 0$, $\omega_2 = 1$, $\omega_3 = 2$ and $\omega_4 = 3$ for the J coefficients in figure 4 and for the I coefficients in figure 5.

Some comments on the usefulness of this scheme in practice are appropriate at this point. The first point to make is that all the BZ integration schemes are intended for problems in which the effort of calculating the $F(\boldsymbol{k})$ and $\omega(\boldsymbol{k})$ is very large. The evaluation

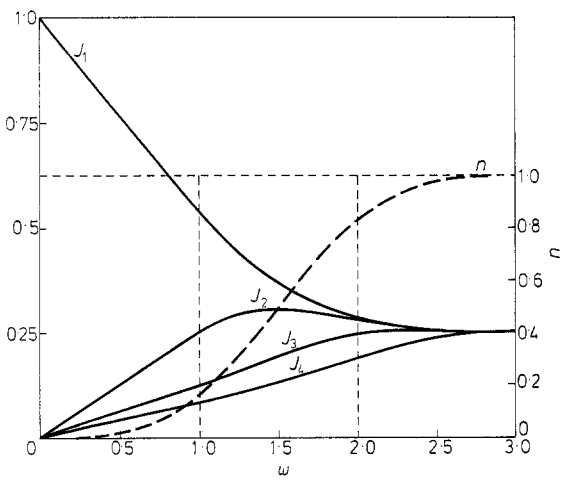

Figure 4. Variation of J_1, J_2, J_3 and J_4 with ω for $\omega_1 = 0$, $\omega_2 = 1$, $\omega_3 = 2$, $\omega_4 = 3$. These coefficients express the averaging of $\tilde{F}(\boldsymbol{k})$ over the occupied portion ($\tilde{\omega}(\boldsymbol{k}) \leqslant \omega$) of the tetrahedral microzone. Also plotted is $n(\omega)$.

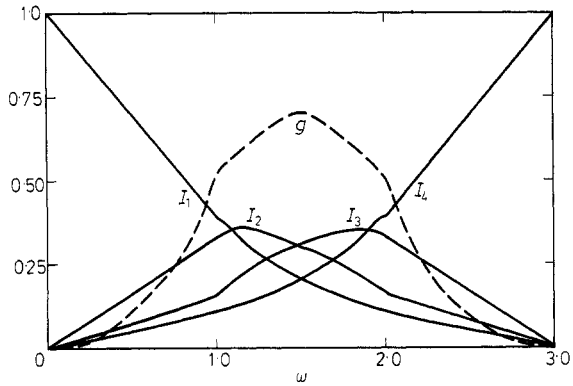

Figure 5. Variation of I_1, I_2, I_3 and I_4 with ω for $\omega_1 = 0$, $\omega_2 = 1$, $\omega_3 = 2$, $\omega_4 = 3$. These coefficients express the averaging of $\tilde{F}(\boldsymbol{k})$ over the planar $\tilde{\omega}(\boldsymbol{k}) = \omega$ surface. Also plotted is $g(\omega)$.

of the I_k and J_k would therefore be an insignificant component of any such calculation and so their rather complicated algebraic expressions should not be construed as a disadvantage. A common method of including matrix element variation in the tetrahedron method is to replace $F(\boldsymbol{k})$ by its value at the centroid of the tetrahedron (Wang and Callaway 1977, Rath and Freeman 1975). The scheme outlined above represents an improvement both in accuracy, since the linear variations in $F(\boldsymbol{k})$ are treated exactly, and in a reduction of the number of $F(\boldsymbol{k})$ evaluations required, since in typical applications of the tetrahedron method there are far fewer vertices than there are tetrahedra.

3. The hybrid tetrahedron method

To apply the tetrahedron method the irreducible region of the BZ must be divided into a sufficiently large number of tetrahedra to obtain results of the desired accuracy. One way of doing this is by successively dividing each tetrahedron into eight smaller tetrahedra in the manner shown in figure 6. We concentrate on a single tetrahedron at some stage in this process and label its vertices by $\boldsymbol{k}_1$, $\boldsymbol{k}_2$, $\boldsymbol{k}_3$ and $\boldsymbol{k}_4$. If the division by eight process is applied twice to this tetrahedron, the additional vertices generated are as shown in figure 7. We note that knowledge of $\omega(\boldsymbol{k})$ and/or $F(\boldsymbol{k})$ at $\boldsymbol{k}_1$ to $\boldsymbol{k}_{10}$, the distinct vertices generated when the division by eight process is applied once to the original tetrahedron, gives sufficient information to provide a unique quadratic representation of $\omega(\boldsymbol{k})$ and/or $F(\boldsymbol{k})$ inside the tetrahedron by requiring the representation to be exact at the points $\boldsymbol{k}_1$ to $\boldsymbol{k}_{10}$. This interpolation can be used to determine the necessary eigenvalues and matrix element values when the tetrahedron method is applied with any larger number of tetrahedra. It is easily seen that this representation of the eigenvalues and matrix elements is continuous throughout the BZ i.e. there is no discontinuity in moving from one tetrahedron to a neighbour.

To simplify the remaining discussion we focus on the evaluation of $g(\omega)$. We believe that this scheme will be most useful when the smaller tetrahedra which will use the quadratically interpolated eigenvalues are generated by successive application of the division by eight process of figure 6. For definiteness we concentrate here on the case in which the division by eight process occurs *once* more. The quadratically interpolated

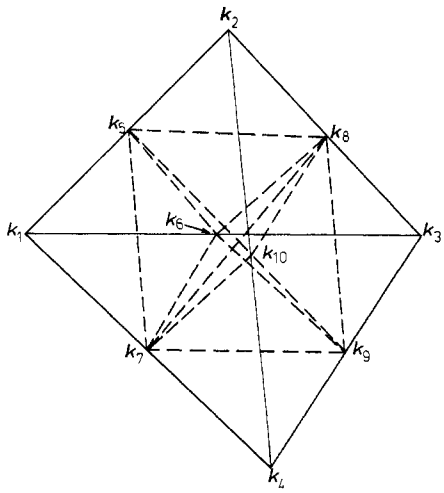

Figure 6. Division of a tetrahedron into eight sub-tetrahedra. The eight tetrahedra have vertices corresponding to the $\boldsymbol{k}$-labels (1, 5, 6, 7), (2, 5, 8, 10), (3, 8, 9, 6), (4, 9, 7, 10), (7, 8, 10, 9), (7, 8, 10, 5), (7, 8, 6, 9) and (7, 8, 6, 5) respectively.

eigenvalues are then required at the points labelled by 11 to 35 in figure 7. The location of the $\boldsymbol{k}$ points of figure 7, expressions for the quadratically interpolated eigenvalues at points 11 to 35 and the 64 equal-volume tetrahedra which result from the division process are listed in tables 1, 2 and 3 respectively. It is an important simplification in practice that the required interpolated eigenvalues are given, in terms of the eigenvalues at

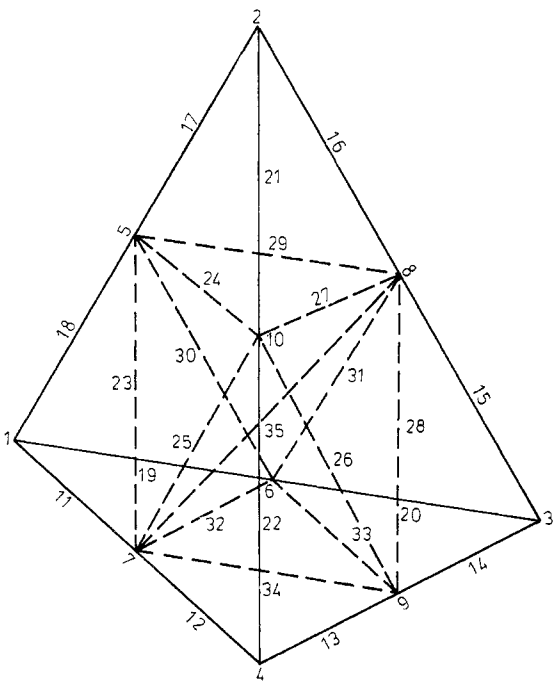

Figure 7. Vertices generated by applying the division by eight process of figure 6 twice.

Table 1. The points labelled by 5 to 35 in figure 7 are simple linear combinations of $\boldsymbol{k}_1$ to $\boldsymbol{k}_4$. In the table below Index is the $\boldsymbol{k}$-vector index and Position indicates the $\boldsymbol{k}$-vector by giving the coefficients of its expansion in terms of $\boldsymbol{k}_1\boldsymbol{k}_4$. For convenience the coefficients have been multiplied by four. For example, the first entry in the left column indicates that $\boldsymbol{k}_5 = (2\boldsymbol{k}_1 + 2\boldsymbol{k}_2)/4$.

Index	Position	Index	Position
5	2(1) + 2(2)	20	1(1) + 3(3)
6	2(1) + 2(3)	21	3(2) + 1(4)
7	2(1) + 2(4)	22	1(2) + 3(4)
8	2(2) + 2(3)	23	2(1) + 1(2) + 1(4)
9	2(3) + 2(4)	24	2(2) + 1(1) + 1(4)
10	2(2) + 2(4)	25	2(4) + 1(1) + 1(2)
11	3(1) + 1(4)	26	2(4) + 1(2) + 1(3)
12	1(1) + 3(4)	27	2(2) + 1(3) + 1(4)
13	3(4) + 1(3)	28	2(3) + 1(2) + 1(4)
14	1(4) + 3(3)	29	2(2) + 1(1) + 1(3)
15	3(3) + 1(2)	30	2(1) + 1(2) + 1(3)
16	1(3) + 3(2)	31	2(3) + 1(1) + 1(2)
17	3(2) + 1(1)	32	2(1) + 1(4) + 1(3)
18	1(2) + 3(1)	33	2(3) + 1(1) + 1(4)
19	3(1) + 1(3)	34	2(4) + 1(1) + 1(3)
		35	1(1) + 1(2) + 1(3) + 1(4)

$\boldsymbol{k}_1$ to $\boldsymbol{k}_{10}$, by simple expressions which are independent of the shape of the original tetrahedron.

We illustrate the use of the scheme by means of a specific example, namely application to the density of states, $g(\epsilon)$, of a single FCC tight-binding band:

$$\epsilon_k = -[\cos(k_x a/2)\cos(k_y a/2) + \cos(k_x a/2)\cos(k_z a/2) + \cos(k_y a/2)\cos(k_z a/2)] \tag{3.1}$$

Jelitto (1969) has evaluated $g(\epsilon)$ for this case, by using special simplifying properties of equation (3.1) to an accuracy of one part in 10^5. For the purpose of comparison we may

Table 2. The quadratically interpolated eigenvalues at the points labelled by 11 to 35 in figure 7 are simple linear combinations of the eigenvalues at $\boldsymbol{k}_1$ to $\boldsymbol{k}_{10}$. The coefficients are given in the same manner as in table 1 and are independent of the shape of the original tetrahedron. For convenience the coefficients have been multiplied by eight.

Index	Eigenvalue	Index	Eigenvalue
11	6(7) + 3(1) − (4)	24	4(5) + 4(10) + 2(7) − (1) − (4)
12	6(7) + 3(4) − (1)	25	4(7) + 4(10) + 2(5) − (1) − (2)
13	6(9) + 3(4) − (3)	26	4(10) + 4(9) + 2(8) − (3) − (2)
14	6(9) + 3(3) − (4)	27	4(10) + 4(8) + 2(9) − (4) − (3)
15	6(8) + 3(3) − (2)	28	4(9) + 4(8) + 2(10) − (2) − (4)
16	6(8) + 3(2) − (3)	29	4(5) + 4(8) + 2(6) − (1) − (3)
17	6(5) + 3(2) − (1)	30	4(5) + 4(6) + 2(8) − (2) − (3)
18	6(5) + 3(1) − (2)	31	4(6) + 4(8) + 2(5) − (1) − (2)
19	6(6) + 3(1) − (3)	32	4(6) + 4(7) + 2(9) − (3) − (4)
20	6(6) + 3(3) − (1)	33	4(6) + 4(9) + 2(7) − (1) − (4)
21	6(10) + 3(2) − (4)	34	4(7) + 4(9) + 2(6) − (1) − (3)
22	6(10) + 3(4) − (2)	35	2(5) + 2(6) + 2(7) + 2(8) + 2(9)
23	4(5) + 4(7) + 2(10) − (2) − (4)		+2(10) − (1) − (2) − (3) − (4)

take his results to be exact. There are Van Hove singularities in $g(\epsilon)$ at $\epsilon = -3$ and at $\epsilon = 0$, reflecting extremal values of ϵ_k at Γ and L respectively. There is also an infinity in $g(\epsilon)$ at $\epsilon = 1$ because of a line of extremal values of ϵ_k from X to W on the FCC BZ surface. The density of states as calculated by Jelitto is plotted in figure 8. We have calculated $g(\epsilon)$ from the tetrahedron method with quadratic interpolation used as described above inside 512 equal-volume tetrahedra into which the irreducible region of the BZ was divided. We refer to the $g(\epsilon)$ corresponding to these tetrahedra, to the 4096

Table 3. The 35 k points in figure 7 are at the vertices of the 64 equal-volume tetrahedra into which the original tetrahedron has been divided. These 64 tetrahedra are listed below by giving the labels of the four k-vectors at the vertices of each tetrahedron.

(1, 18, 19, 11)	(16, 24, 29, 27)	(8, 15, 31, 28)
(30, 18, 19, 11)	(16, 27, 29, 8)	(15, 34, 31, 28)
(5, 18, 23, 30)	(5, 23, 29, 24)	(34, 31, 33, 28)
(18, 11, 30, 23)	(23, 29, 24, 35)	(34, 28, 33, 9)
(6, 19, 30, 32)	(7, 23, 25, 35)	(4, 12, 22, 13)
(11, 30, 32, 23)	(23, 24, 35, 25)	(25, 12, 22, 13)
(11, 19, 30, 32)	(8, 29, 35, 27)	(7, 25, 34, 12)
(11, 32, 23, 7)	(29, 24, 35, 27)	(13, 25, 34, 12)
(8, 29, 31, 35)	(24, 35, 25, 27)	(10, 22, 25, 26)
(30, 29, 31, 35)	(24, 10, 25, 27)	(13, 22, 25, 26)
(5, 29, 23, 30)	(3, 20, 15, 14)	(9, 13, 34, 26)
(29, 35, 30, 23)	(20, 15, 14, 31)	(25, 13, 34, 26)
(6, 31, 30, 32)	(6, 20, 33, 31)	(7, 35, 34, 25)
(35, 31, 30, 32)	(20, 14, 31, 33)	(28, 35, 34, 25)
(35, 30, 23, 32)	(8, 15, 31, 28)	(8, 35, 27, 28)
(35, 32, 23, 7)	(15, 14, 31, 28)	(35, 25, 28, 27)
(2, 17, 21, 16)	(14, 31, 33, 28)	(9, 34, 28, 26)
(24, 17, 21, 16)	(14, 28, 33, 9)	(34, 25, 28, 26)
(5, 17, 29, 24)	(7, 32, 35, 34)	(25, 28, 27, 26)
(17, 16, 29, 24)	(31, 35, 32, 34)	(25, 26, 27, 10)
(10, 21, 24, 27)	(6, 32, 33, 31)	
(21, 16, 24, 27)	(32, 34, 31, 33)	

tetrahedra when the division by eight is applied once, and to the 32 768 tetrahedra when quadratic interpolation is used as $g_1(\epsilon)$, $g_2(\epsilon)$ and $g_3(\epsilon)$ respectively. The average relative errors of $g_1(\epsilon)$, $g_2(\epsilon)$ and $g_3(\epsilon)$ on an equally spaced grid of energy values in the occupied range were found to be 5·7 %, 1·6 % and 0·6 % respectively. The important point to note is that in comparing $g_2(\epsilon)$ and $g_3(\epsilon)$ the reduction in the error is close to the factor of ~ 4 which would be expected if the tetrahedron method were applied directly. In contrast while only 933 'first-principles eigenvalues' were required to obtain $g_3(\epsilon)$ using quadratic interpolation ~ 6000 would be required if the tetrahedron method were applied directly. Further reduction in the error with no additional 'first-principles eigenvalues' would be expected if the division by eight process were applied again with the same quadratic interpolation retained. Alternatively we might expect close to the same accuracy in $g_3(\epsilon)$ using only the 155 first-principles eigenvalues required for $g_1(\epsilon)$ and quadratic interpolation inside 64 tetrahedron in the irreducible region. These observations show that the scheme is quite competitive with that suggested by Chen (1977) who obtained an average relative error in $g(\epsilon)$ of 0·6 % with ~ 400 first-principles eigenvalue determinations for the same test case.

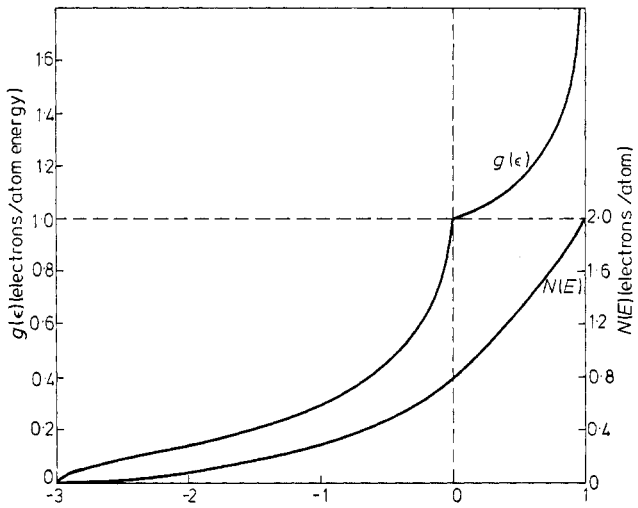

Figure 8. $g(\epsilon)$ for a single tight-binding band in a FCC crystal as given by Jelitto (1969). The units are electrons/(atom energy) and the spin degeneracy factor has been included. Note the Van Hove singularities at $\epsilon = -3$ and $\epsilon = 0$ and the divergence of $g(\epsilon)$ *at* $\epsilon = 1$.

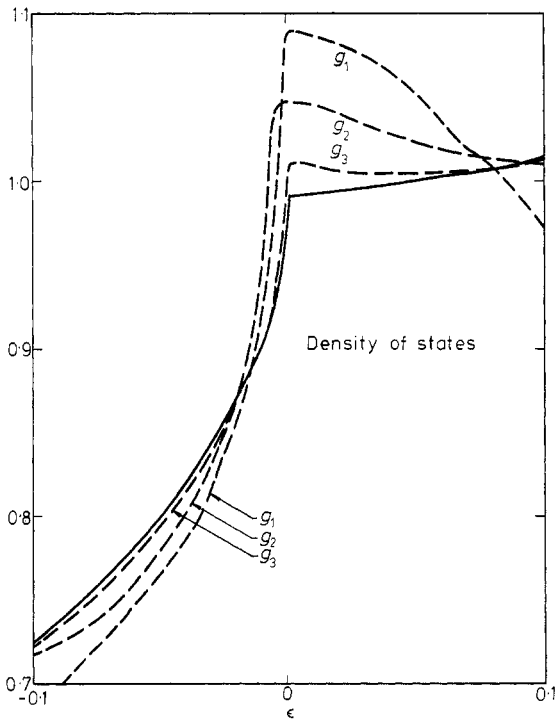

Figure 9. $g_1(\epsilon)$, $g_2(\epsilon)$ and $g_3(\epsilon)$ near the Van Hove singularity at $\epsilon = 0$. The solid line is the exact result as given by Jelitto (1969). The units are electron/(atom energy) and the spin degeneracy factor has been included.

The quadratic interpolation tetrahedron method was also found to give a more accurate $g(\epsilon)$ near Van Hove singularities, as is illustrated by figure 9, thus controlling one of the disadvantages of linear analytic schemes. Both a reduced error at the singular energy and a reduced region of relatively high error near the singularity were achieved with no additional first-principles eigenvalues.

4. Concluding remarks

The tetrahedron method has proved to be a useful BZ integration scheme for evaluating spectral properties of solids. In this paper we have extended the usefulness of the method by providing simple and convenient expressions for including matrix element variation in the tetrahedron method and by illustrating how quadratic interpolation may be used to accelerate its convergence. Both aspects have proved useful in applications to Pd and Pt (Liu *et al* 1979). For example, the matrix element variation capability is useful in accounting for the oscillations of the Fermi surface in the iterative approach to self-consistency in self-consistent band calculations and in calculating the form factors of the induced magnetisation in paramagnetic metals. On the other hand, quadratic interpolation may be used with the tetrahedron method to provide improved accuracy for a given number of first principles matrix elements and eigenvalue evaluations.

Acknowledgment

The authors wish to acknowledge informative and stimulating discussions with Dr L Wilk concerning quadratic interpolation for electronic energy bands.

References

Blackman W 1939 *Proc. R. Phys. Soc.* **A159** 416
Brust 1968 *Comput. Phys.* **8** 33
Chen A 1977 *Phys. Rev.* B **16** 3291
Cooke J F and Wood R F 1972 *Phys. Rev.* B **5** 1276
Gilat G 1972 *J. Comput. Phys.* **10** 432
—— 1976 *Methods Comput. Phys.* **15** 317
Gilat G and Bharatiya N R 1975 *Phys. Rev.* B **12** 3479
Gilat G and Dolling G 1964 *Phys. Lett.* **22** 715
Gilat G and Raubenheimer L J 1966 *Phys. Rev.* **144** 390
Janak J R, Eastman D E and Williams A R 1970 *Solid St. Commun.* **8** 271
Jelitto R J 1969 *J. Phys. Chem. Solids* **20** 609
Jepsen O and Andersen O K 1971 *Solid St. Commun.* **9** 1763
Lehmann G and Taut M 1972 *Phys. Stat. Solidi* b **54** 469
Liu K L, MacDonald A H, Daams J M, Vosko S H and Koelling D D 1979 *J. Magn. Mater.* to be published
Mueller F M, Garland J W, Cohen M H and Benneman K H 1971 *Ann. Phys. NY* **67** 19
Rath J and Freeman A J 1975 *Phys. Rev.* B **11** 2109
Wang C S and Callaway J 1977 *Phys. Rev. B* **15** 298